Multi-stream transmission for highly frequency selective channels in MIMO-FBMC/OQAM systems

Màrius Caus*, *Student Member, IEEE,* and Ana I. Pérez-Neira, *Senior Member, IEEE*

***Abstract*—This paper addresses the joint design of MIMO precoding and decoding matrices for filter bank multicarrier (FBMC) systems based on OQAM, known as FBMC/OQAM. Existing solutions that support multi-stream transmission only give satisfactory performance in scenarios with high coherence bandwidth channels. By contrast, the schemes that do not make any assumptions about the flatness of the channel do not allow the allocation of multiple streams per-subband. To make progress towards the application of FBMC/OQAM to MIMO channels, we study the design of novel solutions that could simultaneously provide robustness against the channel frequency selectivity and support multi-stream transmission. To this end, two techniques have been devised under the criterion of minimizing the sum mean square error. The non-circular nature of the OQAM symbols has not been ignored, making evident the convenience of performing a widely linear processing. The first technique keeps the complexity at a reasonable level, which is practical from the implementation point of view as it is not iterative, but in exchange the original problem is relaxed yielding a suboptimal solution. With the objective of performing closer to the optimum solution, the second option iteratively computes precoders and equalizers by resorting to an alternating optimization method, which is much more complex. We have demonstrated via simulations that the first technique nearly achieves the same results as the iterative design. Simulation results show that the proposed low-complexity solution outperforms existing MIMO-FBMC/OQAM schemes in terms of bit error rate (BER). As for the comparison with OFDM, the numerical results highlight that FBMC/OQAM remains competitive, with and without perfect channel state information, while it provides spectral efficiency gains. Under highly frequency selective channels the proposed technique significantly outperforms OFDM.**

***Index Terms*—MIMO precoder/decoder design, multi-stream transmission, OFDM, and FBMC based on OQAM.**

I. Introduction

In this work we study the joint design of transmit and receive beamformers for frequency selective multiple-input-multiple-output (MIMO) channels. With respect to the figure of merit that governs the design, we consider the minimization of the sum mean square error (MSE) subject to a power constraint. Since this topic has been widely studied over the recent years we review right after the different approaches that have been proposed to tackle the problem. In this sense, we first introduce a narrowband point-to-point MIMO communication system, where the transmitter and the receiver are equipped with N_T and N_R antennas, respectively. At the nth channel access the system equation is $\check{\mathbf{d}}[n] = \mathbf{A}^H\mathbf{H}\mathbf{B}\mathbf{d}[n] + \mathbf{A}^H\mathbf{w}[n]$. The vector of symbols $\mathbf{d}[n] \in \mathbb{C}^{S\times 1}$ is pre-processed with the precoder $\mathbf{B} \in \mathbb{C}^{N_T\times S}$ and it is post-processed with the equalizer $\mathbf{A} \in \mathbb{C}^{N_R\times S}$. Note that S streams are simultaneously transmitted. The vector $\mathbf{w}[n] \in \mathbb{C}^{N_R\times 1}$ models the additive noise samples that contaminate each receiver chain and the matrix $\mathbf{H} \in \mathbb{C}^{N_R\times N_T}$ gathers the channel coefficients that characterize the links between any transmitter and receiver antenna pairs. According to the system model, the optimization problem that is proposed reduces to

$$\begin{aligned} &\underset{\mathbf{A},\mathbf{B}}{\operatorname{argmin}}\, \mathbb{E}\left\{\left\|\check{\mathbf{d}}[n] - \mathbf{d}[n]\right\|_2^2\right\} \\ &s.t.\ \ \mathbb{E}\left\{\|\mathbf{B}\mathbf{d}[n]\|_2^2\right\} \leq P_T. \end{aligned} \tag{1}$$

The restriction imposed on the average transmitted power ensures that the problem is well-posed. In this sense, the maximum allowable transmit power is given by P_T. The solution of (1) can be computed when the channel state information (CSI) is known at both ends of the link, see e.g. [1], [2]. When the channel has memory it is mandatory to carry out a different processing than [1], [2].

One alternative is to operate on a block-by-block fashion, [3]. To avoid inter-block interference (IBI) a guard interval (GI) is inserted before the transmission of the next block. If the receiver stacks the snapshots obtained when the transmitter is not idle, then the optimization problem is the one in (1) with a channel matrix that is block Toeplitz. In order not to sacrifice rate, the precoder and the equalizer have to diagonalize the MIMO channel transfer function. To do so, it is required to perform a broadband singular value decomposition (BSVD) of the polynomial channel matrix, [4]. Since the resulting independent subchannels are frequency selective it is deemed necessary to further process the signals to eliminate the residual inter-symbol interference (ISI).

Another alternative to deal with the frequency selectivity of the channel consists in partitioning the band into narrower subchannels. In this respect, the most prominent multicarrier modulation is the so-called orthogonal frequency division multiplexing (OFDM). The beauty of this technique stems from the fact that the end-to-end system can be modeled as a set of parallel flat fading channels thanks to the transmission of a cyclic prefix (CP). This enables us to pre- and post-process the symbols on a per-subcarrier basis as follows:

$$\check{\mathbf{d}}_q[k] = \mathbf{A}_q^H\mathbf{H}_q\mathbf{B}_q\mathbf{d}_q[k] + \mathbf{A}_q^H\mathbf{w}_q[k], \quad q = 0, ..., M-1, \tag{2}$$

where M is the number of subbands. Now $\mathbf{H}_q$ accounts for the MIMO channel transfer function evaluated on the radial

M. Caus is with the Department of Signal Theory and Communications, Universitat Politècnica de Catalunya (UPC), 08034 Barcelona, Spain (e-mail: marius.caus@upc.edu).

A.I. Pérez-Neira is with the Department of Signal Theory and Communications, Universitat Politècnica de Catalunya (UPC), 08034 Barcelona, Spain and with the Centre Tecnològic de Telecomunicacions de Catalunya (CTTC), 08860 Castelldefels, Barcelona, Spain (e-mail: ana.isabel.perez@upc.edu).

frequency $\frac{2\pi}{M}q$. Unlike the single carrier case the optimization problem in the multicarrier context boils down to solve

$$\begin{aligned} &\underset{\{\mathbf{A}_q,\mathbf{B}_q\}}{\operatorname{argmin}} \sum_{q=0}^{M-1} \mathbb{E}\left\{\left\|\check{\mathbf{d}}_q[k]-\mathbf{d}_q[k]\right\|_2^2\right\} \\ &s.t. \quad \sum_{q=0}^{M-1} \mathbb{E}\left\{\|\mathbf{B}_q\mathbf{d}_q[k]\|_2^2\right\} \leq P_T. \end{aligned} \tag{3}$$

The authors in [5] have developed a framework that enables us to solve (3). At the expense of increasing the computational complexity, the performance can be improved by jointly processing all the subbands as [3], [5] detail. To overcome the signal to noise ratio loss, which is due to the CP transmission, the authors in [6] have proposed the utilisation of the filtered multitone (FMT) modulation, [7]. The main difference with respect to OFDM is that the subcarrier signals decay faster in the frequency domain than the sinc-shaped filter. However, both OFDM and FMT systems suffer a bandwidth loss. In the OFDM case, the loss has to do with the CP transmission. In the FMT modulation, although no redundancy is transmitted a guard band between subcarriers is inserted to ensure that there is no overlapping, which results in a spectral efficiency loss. If maximum bandwidth efficiency is desired, then the filter bank multicarrier modulation based on the offset quadrature amplitude modulation (FBMC/OQAM) is the best alternative [8]. This scheme was first introduced by Saltzberg in [9]. The efficient implementation of FBMC/OQAM as well as the perfect reconstruction property are derived in [10].

With the aim of exploiting the spatial diversity without sacrificing the rate, we propose combining MIMO precoding and decoding techniques with FBMC/OQAM. To the best of authors' knowledge the work derived in [11] is one of the few publications that have studied the design of MIMO precoding and decoding techniques in the FBMC/OQAM context. The results in [11] confirm that the solution gives a satisfactory performance in scenarios where the channel coherence bandwidth exceeds the subcarrier spacing. However, when the channel frequency selectivity becomes stronger the bit error rate (BER) plots exhibit an error floor [11]. To remedy it, the authors in [12] propose a joint transmitter and receiver beamforming design that is ISI and inter-carrier interference (ICI) aware, which makes the system more robust to the channel frequency selectivity than [11]. Nevertheless, the scheme is only able to accommodate a single stream per-subband for a fixed power allocation. It must be mentioned that most of the existing solutions that combine multi-stream techniques with the FBMC/OQAM modulation solely resort to the CSI at the receiver, see e.g. [13]–[23].

As a summary the contributions of this paper are as follows:

- We design MIMO precoding and decoding matrices with the objective of transmitting several streams on a per-subcarrier basis in the FBMC/OQAM context. In this sense, two different designs have been described. The first one aims at keeping the complexity low. To this end, the original problem is relaxed and, therefore, the solution is suboptimal. In the second case, we are able to find a local optimal solution. However, the complexity is drastically increased because the solution is based on the alternating optimization method. In both cases, we make no assumptions about the flatness of the channel and we exploit the non-circular nature exhibited by the OQAM symbols by performing a widely linear (WL) processing.
- We have carried out an analysis of the quality of the links after pre- and post-processing the symbols when the non-iterative technique is applied. The analysis reveals in which multi-antenna configurations the FBMC/OQAM modulation scheme may remain competitive with OFDM.

The rest of the paper is organized as follows. Section II formulates the expressions involved in MIMO-FBMC/OQAM systems. In Section III, we devise a new subband processing that supports multi-stream transmission for the MIMO-FBMC/OQAM scheme. Additionally, we have carried out an analysis of the quality of the links. In Section IV, we propose to minimize the sum MSE by resorting to an alternating optimization method. The numerical results are included in Section V and finally Section VI draws the conclusions.

Notation: Upper case boldfaced letters denote matrices and lower case boldfaced letters denote vectors. Let the superscripts $(.)^T$, $(.)^*$ and $(.)^H$ denote transpose, complex conjugate and Hermitian operations, respectively. We will use $[\mathbf{A}]_{ij}$ to refer to the (*i*th, *j*th) element of matrix $\mathbf{A}$. By $\mathbf{I}_N$ we denote the N-dimensional identity matrix. We define $\lambda_l(\mathbf{A})$ to be the *l*th largest eigenvalue of matrix $\mathbf{A}$. We define diag $\{a_1, ..., a_N\}$ to be a $N \times N$ diagonal matrix, where the (*k*th, *k*th) element is given by a_k. We will use $*$ to denote the convolution operation.

II. MIMO-FBMC/OQAM SYSTEM MODEL

In this work we focus on the FBMC/OQAM modulation, [10]. We consider a multi-antenna configuration that consists of deploying N_T antennas at transmission and N_R antennas at reception. The resulting superimposed signal at the *i*th ($1 \leq i \leq N_T$) transmit antenna output is given by

$$s_i[n] = \sum_{k=-\infty}^{\infty} \sum_{m=0}^{M-1} v_{im}[k] f_m\left[n - k\frac{M}{2}\right] \tag{4}$$

$$f_m[n] = p[n] e^{j\frac{2\pi}{M}m\left(n-\frac{L-1}{2}\right)} \tag{5}$$

where $p[n]$ is the prototype pulse, which has a length equal to L. Note that the subband filters $\{f_m[n]\}$ are used to build the synthesis filter bank (SFB), which allows us to partition the band into M subchannels. The precoded symbol is expressed as follows: $v_{im}[k] = \sum_{r=1}^{S} b_{im}^r x_m^r[k]$, which highlights that *S* streams are spatially multiplexed over each subcarrier. Let $\{b_{im}^r\}$ be the coefficients of the precoders and $x_m^r[k]$ be the *r*th stream multiplexed on the *m*th subband. Since the transmitted symbols are modulated according to the OQAM scheme, it is possible to factorize $x_m^r[k]$ as the product of the real PAM symbol $d_m^r[k]$ and the phase term $\theta_m[k]$, i.e. $x_m^r[k] = d_m^r[k]\theta_m[k]$. The phase term is defined as

$$\theta_m[k] = \begin{cases} 1 & m+k \text{ even} \\ j & m+k \text{ odd} \end{cases} \tag{6}$$

to ensure that the frequency shift between adjacent symbols in the time-frequency grid is $\frac{\pi}{2}$. To differentiate between low-

and high-rate signals we have used different sampling indexes. In this sense, the index *k* is used by the low-rate signals while the high-rate signals utilize the index *n*.

The received signal at the input of the *j*th receive antenna is contaminated by additive noise and degraded by multipath fading. As a result, the signal received by the *j*th antenna is

$$r_j[n] = \sum_{i=1}^{N_T} s_i[n] * h_{ij}[n] + w_j[n], \quad j = 1, ..., N_R, \tag{7}$$

where $w_j[n]$ denotes the noise samples of the *j*th receive antenna and the term $h_{ij}[n]$ refers to the channel impulse response associated to the transmitter *i* and the receiver *j*. To demultiplex the low-rate signals, the received signal is passed through a bank of matched filters, whose outcomes are downsampled by the factor $M/2$, yielding

$$y_q^j[k] = \left(r_j[n] * f_q^*[-n]\right)_{\downarrow M/2}, \tag{8}$$

for $1 \leq j \leq N_R$ and $0 \leq q \leq M-1$. As for the mathematical notation, the expression $(.)_{\downarrow x}$ performs a decimation by a factor of *x*. Unlike the processing carried out at the transmit side, now the matched filters $\left\{f_q^*[-n]\right\}$ are used to build the analysis filter bank (AFB). Bearing in mind (4), the AFB outputs can be compactly formulated as

$$y_q^j[k] = \sum_{m=q-1}^{q+1} \sum_{i=1}^{N_T} v_{im}[k] * g_{qm}^{ij}[k] + w_q^j[k] \tag{9}$$

$$g_{qm}^{ij}[k] = \left(f_m[n] * h_{ij}[n] * f_q^*[-n]\right)_{\downarrow M/2} \tag{10}$$

$$w_q^j[k] = \left(w_j[n] * f_q^*[-n]\right)_{\downarrow M/2}. \tag{11}$$

Note that ICI exclusively comes from the most immediate neighbors thanks to the good confinement of the pulses in the frequency plane, see e.g. [10], [24], [25]. In the same line, we assume that only the first and the second order neighbours bring about ISI. As a consequence, $g_{qm}^{ij}[k] \neq 0$ for $-2 \leq k \leq 2$. In order to enhance the quality of the estimates, the demodulated data is further processed on a per-subcarrier basis by means of a broadband MIMO equalizer. This means that on the *q*th subcarrier the multi-tap equalizers $\left\{a_{1q}^l[k], ..., a_{N_Rq}^l[k]\right\}$, which are different from zero for $-L_a \leq k \leq L_a$, are responsible for performing the receive processing that is aimed at recovering the stream $d_q^l[k]$. Then, it follows that the PAM symbols are estimated by compensating the phase term and extracting the real part of the equalized signals, which boils down to operate as follows:

$$\check{d}_q^l[k] = \Re\left(u_q^l[k]\right), \quad l = 1, ..., S, \quad q = 0, ..., M-1, \tag{12}$$

$$u_q^l[k] = \theta_q^*[k] \left(\sum_{j=1}^{N_R} \left(a_{jq}^l[k]\right)^* * y_q^j[k] \right). \tag{13}$$

Plugging (9) into (13) results in

$$\begin{aligned} u_q^l[k] = \theta_q^*[k] \Bigg(& \sum_{j=1}^{N_R} \left(a_{jq}^l[k]\right)^* * w_q^j[k] + \\ & \sum_{m=q-1}^{q+1} \sum_{j=1}^{N_R} \sum_{i=1}^{N_T} \left(a_{jq}^l[k]\right)^* * v_{im}[k] * g_{qm}^{ij}[k] \Bigg). \end{aligned} \tag{14}$$

A. Compact formulation

The problem of devising transmit and receive matrices directly from (12) and (14) is difficult. To get a more tractable expression we use this equality

$$\begin{aligned} & \sum_{i=1}^{N_T} \left(a_{jq}^l[k]\right)^* * v_{im}[k] * g_{qm}^{ij}[k] = \\ & \sum_{t=-L_a-2}^{L_a+2} \theta_m[k-t] \left(\mathbf{a}_{jq}^l\right)^H \mathbf{G}_{qm}^j[t] \mathbf{B}_m \mathbf{d}_m[k-t] \end{aligned} \tag{15}$$

where $\mathbf{a}_{jq}^l = \left[a_{jq}^l[-L_a], ..., a_{jq}^l[L_a]\right]^T$,

$$\mathbf{G}_{qm}^j[t] = \begin{bmatrix} g_{qm}^{1j}[t+L_a] & \cdots & g_{qm}^{N_Tj}[t+L_a] \\ \vdots & & \vdots \\ g_{qm}^{1j}[t-L_a] & \cdots & g_{qm}^{N_Tj}[t-L_a] \end{bmatrix} \tag{16}$$

$$\mathbf{B}_m = \begin{bmatrix} b_{1m}^1 & . & b_{1m}^S \\ \vdots & . & \vdots \\ b_{N_Tm}^1 & . & b_{N_Tm}^S \end{bmatrix} \tag{17}$$

and $\mathbf{d}_m[k] = \left[d_m^1[k] ... d_m^S[k]\right]^T$. Note that L_a determines the length of $\mathbf{a}_{jq}^l$, which is equal to $1 + 2L_a$. With the aim of alleviating the complexity, the precoder has been restricted to be real-valued and to have a single-tap. The reason why we have discarded the alternative configuration where both MIMO precoding and decoding matrices are complex-valued is further justified at the end of this section. Now, plugging (15) into (14) leads to

$$\begin{aligned} u_q^l[k] = \theta_q^*[k] \Bigg(& \sum_{m=q-1}^{q+1} \sum_{t=-L_a-2}^{L_a+2} \theta_m[k-t] \left(\mathbf{a}_q^l\right)^H \\ & \times \mathbf{G}_{qm}[t] \mathbf{B}_m \mathbf{d}_m[k-t] \Bigg) + \left(\mathbf{a}_q^l\right)^H \mathbf{w}_q[k], \end{aligned} \tag{18}$$

where the noise vector is written as

$$\begin{aligned} \mathbf{w}_q[k] \quad = & \theta_q^*[k] \left[w_q^1[k+L_a] \dots w_q^1[k-L_a] \right. \\ & \left. \dots w_q^{N_R}[k+L_a] \dots w_q^{N_R}[k-L_a]\right]^T. \end{aligned} \tag{19}$$

To get (18) we define $\mathbf{a}_q^l = \left[\left(\mathbf{a}_{1q}^l\right)^T ... \left(\mathbf{a}_{N_Rq}^l\right)^T\right]^T$ and $\mathbf{G}_{qm}[t] = \left[\left(\mathbf{G}_{qm}^1[t]\right)^T ... \left(\mathbf{G}_{qm}^{N_R}[t]\right)^T\right]^T$. As the subcarrier model that is depicted in Fig. 1 highlights, the symbol detection is sensitive to be affected by ISI and ICI and thus the precoders and the equalizers have to be interference aware, which complicates the design. Defining $\mathbf{E}_{qm}^k[t] = \left(\theta_q^*[k]\theta_m[k-t]\right) \mathbf{G}_{qm}[t]$, then (18) becomes

$$\begin{aligned} u_q^l[k] = & \sum_{m=q-1}^{q+1} \sum_{t=-L_a-2}^{L_a+2} \left(\mathbf{a}_q^l\right)^H \mathbf{E}_{qm}^k[t] \mathbf{B}_m \mathbf{d}_m[k-t] \\ & + \left(\mathbf{a}_q^l\right)^H \mathbf{w}_q[k]. \end{aligned} \tag{20}$$

Let $\mathbf{a}$ be either a matrix or a vector, we can define the extended notation by stacking column-wise the real and imaginary components, i.e. $\mathbf{a}_e = \left[\Re\left(\mathbf{a}^T\right) \quad \Im\left(\mathbf{a}^T\right)\right]^T$. This enables

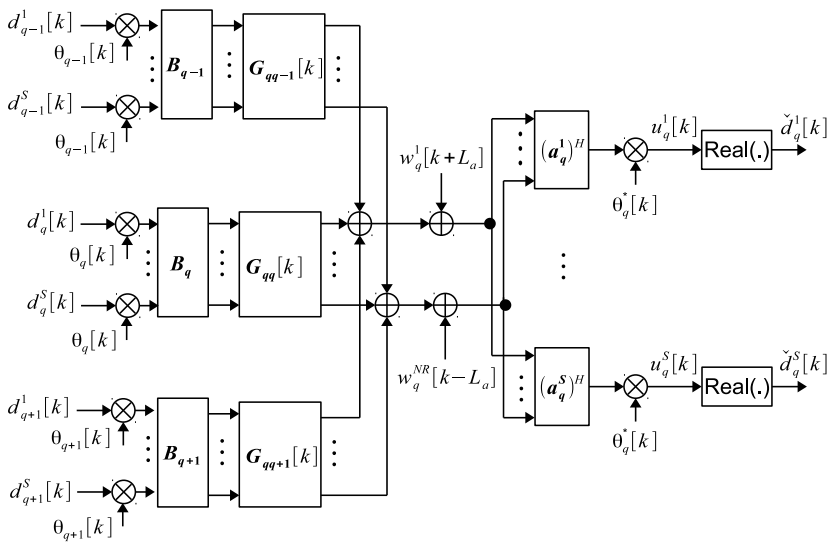

Figure 1. Subcarrier model of the MIMO-FBMC/OQAM scheme.

us to formulate the estimated real PAM symbols as follows:

$$\check{d}_q^l[k] = \sum_{m=q-1}^{q+1} \sum_{t=-L_a-2}^{L_a+2} \left(\mathbf{a}_{q,e}^l\right)^T \mathbf{E}_{qm,e}^k[t]\mathbf{B}_m\mathbf{d}_m[k-t] + \left(\mathbf{a}_{q,e}^l\right)^T \mathbf{w}_{q,e}[k]. \tag{21}$$

At this point it is reasonable to question why precoders are restricted to be real-valued. By examining (20) and (21) we can assert that if precoders are complex-valued, then there are more degrees of freedom at the transmit side whereas the number of interference terms in (21) increases. Thus, at first glance it is not obvious to foresee if complex-valued precoders are advantageous. However, we have empirically observed that the suboptimal processing proposed in Section III yields the lowest BER when precoders solely have in-phase components, thus supporting the use of real-valued precoders. It seems that the good behaviour exhibited by the real-valued precoders is related to the optimization procedure described in Section III and the OQAM.

In order to exploit the non-circular nature exhibited by the OQAM symbols we have adopted a real-valued representation. By examining (21) it becomes noticeable that real and imaginary parts are independently processed giving rise to WL filtering [26]. In other words, (21) depends linearly on the real and the imaginary parts of the equalizer inputs. Note that the structure of the proposed receiver hinges on the use of real-valued equalizers the length of which is two-fold with respect to the complex-valued linear counterpart. As a result, there is no penalty in terms of complexity for treating real and imaginary parts separately. Therefore, WL filters are as attractive as linear filters to devise low-complexity solutions.

III. Joint transmitter and receiver design

In this section we devise a new subband processing that supports multi-stream transmission in MIMO-FBMC/OQAM systems. Since the required complexity to solve the original problem may render the solution impractical, we have relaxed the problem. This strategy poses a simpler problem to be solved but the solution is suboptimal. For this reason we have carried out an analysis of the quality of the links to determine in which multi-antenna configurations FBMC/OQAM and OFDM may give similar performance.

A. Suboptimal subband processing

In this subsection we study how to jointly design transmit and receive processing when perfect CSI is available. Regarding the optimization criterion, we opt for the minimization of the sum MSE. Defining the MSE of the *l*th stream transmitted on the *q*th subband as $MSE_q^l = \mathbb{E}\left\{\left|d_q^l[k] - \check{d}_q^l[k]\right|^2\right\}$, the problem to be solved is

$$\begin{aligned} &\underset{\left\{\mathbf{a}_{q,e}^l, \mathbf{B}_q\right\}}{\operatorname{argmin}} \sum_{q=0}^{M-1}\sum_{l=1}^{S} MSE_q^l \\ &s.t. \quad \sum_{q=0}^{M-1} \mathbb{E}\left\{\left\|\mathbf{B}_q\mathbf{d}_q[k]\right\|_2^2\right\} = \sum_{q=0}^{M-1} \left\|\mathbf{B}_q\right\|_F^2 \leq P_T, \end{aligned} \tag{22}$$

where $\left\|\mathbf{B}_q\right\|_F^2 = \operatorname{tr}\left(\mathbf{B}_q\mathbf{B}_q^H\right)$. We use $\operatorname{tr}\left(\mathbf{B}_q\mathbf{B}_q^H\right)$ to denote the trace of $\mathbf{B}_q\mathbf{B}_q^H$. Note that we have assumed that symbols are independent and have unit-energy, i.e. $\mathbb{E}\left\{\left|d_m^l[k]d_q^s[n]\right|^2\right\} = \delta_{l,s}\delta_{m,q}\delta_{n,k}$. Then, the MSE can be formulated as

$$\begin{aligned} MSE_q^l &= 1 + \sum_{m=q-1}^{q+1} \sum_{t=-L_a-2}^{L_a+2} \left\|\left(\mathbf{a}_{q,e}^l\right)^T \mathbf{E}_{qm,e}^k[t]\mathbf{B}_m\right\|_2^2 \\ &\quad + \left(\mathbf{a}_{q,e}^l\right)^T \mathbf{R}_q\mathbf{a}_{q,e}^l - 2\left(\mathbf{a}_{q,e}^l\right)^T \mathbf{E}_{qq,e}^k[0]\mathbf{B}_q\mathbf{e}_l. \end{aligned} \tag{23}$$

In notation terms the unitary vector $\mathbf{e}_l$ is zero-valued except in the *l*th position. The noise correlation matrix is given by $\mathbf{R}_q = \mathbb{E}\left\{\mathbf{w}_{q,e}[k]\mathbf{w}_{q,e}^T[k]\right\}$. The analytical expression can be found in [12]. It can be readily checked that the MSE is independent of k and, therefore, the same metric is used for k odd and k even. Due to the ICI we cannot decouple the problem into M disjoint problems. This highlights that some relaxation has to be applied if we want to alleviate the complexity of the

$$MSE_q^l \leq MSE_{lq}^{UB} = \; 1+\sum_{\substack{m=q-1\\ m\neq q}}^{q+1}\sum_{t=-L_a-2}^{L_a+2}\lambda_1\left(\mathbf{B}_m\mathbf{B}_m^T\right)\left\|\left(\mathbf{a}_{q,e}^l\right)^T\mathbf{E}_{qm,e}^k[t]\right\|_2^2+\sum_{\substack{t=-L_a-2\\ t\neq 0}}^{L_a+2}\lambda_1\left(\mathbf{B}_q\mathbf{B}_q^T\right)\left\|\left(\mathbf{a}_{q,e}^l\right)^T\mathbf{E}_{qq,e}^k[t]\right\|_2^2 + \left\|\left(\mathbf{a}_{q,e}^l\right)^T\mathbf{E}_{qq,e}^k[0]\mathbf{B}_q\right\|_2^2+\left(\mathbf{a}_{q,e}^l\right)^T\mathbf{R}_q\mathbf{a}_{q,e}^l-2\left(\mathbf{a}_{q,e}^l\right)^T\mathbf{E}_{qq,e}^k[0]\mathbf{B}_q\mathbf{e}_l. \tag{24}$$

optimization procedure. In this sense, we propose to substitute the objective function of (23) by the upper bound of (24). Note that (24) hinges on the well-known inequality $\text{tr}\left(\mathbf{AB}\right)\leq\sum_{i=1}^{N}\lambda_i\left(\mathbf{A}\right)\lambda_i\left(\mathbf{B}\right)$, where $\mathbf{A}$ and $\mathbf{B}$ are two $N\times N$ positive semidefinite Hermitian matrices, [27]. The terms $\lambda_i\left(\mathbf{A}\right)$ and $\lambda_i\left(\mathbf{B}\right)$ account for the eigenvalues of $\mathbf{A}$ and $\mathbf{B}$, respectively, which are arranged in descending order. Taking into account that $\text{rank}=\left(\mathbf{E}_{qm,e}^k[t]\right)^T\mathbf{a}_{q,e}^l\left(\mathbf{a}_{q,e}^l\right)^T\mathbf{E}_{qm,e}^k[t]=1$ along with the invariance of the trace with the order of the multiplication, leads to this result

$$\left\|\left(\mathbf{a}_{q,e}^l\right)^T\mathbf{E}_{qm,e}^k[t]\mathbf{B}_m\right\|_2^2\leq\lambda_1\left(\mathbf{B}_m\mathbf{B}_m^T\right)\left\|\left(\mathbf{a}_{q,e}^l\right)^T\mathbf{E}_{qm,e}^k[t]\right\|_2^2. \tag{25}$$

With the aim of further simplifying the problem we assume that the dominant eigenvalue of $\mathbf{B}_m\mathbf{B}_m^T$ is upper bounded as follows: $\lambda_1\left(\mathbf{B}_m\mathbf{B}_m^T\right)\leq b_m$. This assumption opens the door to work with a new performance metric, which is defined as

$$\begin{aligned}UB_q^l=1+&\sum_{\substack{m=q-1\\ m\neq q}}^{q+1}\sum_{t=-L_a-2}^{L_a+2}b_m\left\|\left(\mathbf{a}_{q,e}^l\right)^T\mathbf{E}_{qm,e}^k[t]\right\|_2^2+\\ &\sum_{\substack{t=-L_a-2\\ t\neq 0}}^{L_a+2}b_q\left\|\left(\mathbf{a}_{q,e}^l\right)^T\mathbf{E}_{qq,e}^k[t]\right\|_2^2+\left\|\left(\mathbf{a}_{q,e}^l\right)^T\mathbf{E}_{qq,e}^k[0]\mathbf{B}_q\right\|_2^2\\ &+\left(\mathbf{a}_{q,e}^l\right)^T\mathbf{R}_q\mathbf{a}_{q,e}^l-2\left(\mathbf{a}_{q,e}^l\right)^T\mathbf{E}_{qq,e}^k[0]\mathbf{B}_q\mathbf{e}_l.\end{aligned} \tag{26}$$

Then, the new minimization problem becomes

$$\begin{aligned}&\underset{\left\{\mathbf{a}_{q,e}^l,\mathbf{B}_q\right\}}{\text{argmin}}\sum_{q=0}^{M-1}\sum_{l=1}^{S}UB_q^l\\ &s.t.\quad\sum_{q=0}^{M-1}\left\|\mathbf{B}_q\right\|_F^2\leq P_T\\ &\qquad\lambda_1\left(\mathbf{B}_q\mathbf{B}_q^T\right)\leq b_q,\quad 0\leq q\leq M-1.\end{aligned} \tag{27}$$

It is important to remark that $MSE_q^l\leq MSE_{lq}^{UB}\leq UB_q^l$ if $\lambda_1\left(\mathbf{B}_q\mathbf{B}_q^T\right)\leq b_q$. As a consequence, (27) minimizes an upper bound of the sum MSE. As we will show in the following, the expressions that come into play when solving (27) offer a good analytical tractability, which is of paramount importance to formulate a solution in a closed-form expression. Towards this end, we propose to apply the two-step algorithm described in [5] to obtain the precoding matrices $\{\mathbf{B}_q\}$ and the receive vectors $\left\{\mathbf{a}_{q,e}^l\right\}$. The first problem to be solved is given by

$$\underset{\left\{\mathbf{a}_{q,e}^l\right\}}{\text{argmin}}\sum_{q=0}^{M-1}\sum_{l=1}^{S}UB_q^l. \tag{28}$$

For a fixed transmit processing the problem (28) is convex, thus the optimal equalizers are written in this form

$$\mathbf{a}_{q,e}^l=\left(\mathbf{C}_q+\mathbf{E}_{qq,e}^k[0]\mathbf{B}_q\left(\mathbf{E}_{qq,e}^k[0]\mathbf{B}_q\right)^T\right)^{-1}\mathbf{E}_{qq,e}^k[0]\mathbf{B}_q\mathbf{e}_l \tag{29}$$

with

$$\begin{aligned}\mathbf{C}_q=&\sum_{\substack{m=q-1\\ m\neq q}}^{q+1}\sum_{t=-L_a-2}^{L_a+2}b_m\mathbf{E}_{qm,e}^k[t]\left(\mathbf{E}_{qm,e}^k[t]\right)^T\\ &+\sum_{\substack{t=-L_a-2\\ t\neq 0}}^{L_a+2}b_q\mathbf{E}_{qq,e}^k[t]\left(\mathbf{E}_{qq,e}^k[t]\right)^T+\mathbf{R}_q.\end{aligned} \tag{30}$$

In the second step of the algorithm, the receive vectors in (26) are particularized for (29) and the transmit matrices are optimized so that the upper bound on the sum MSE is minimized. Thus, the problem reduces to

$$\begin{aligned}&\underset{\{\mathbf{B}_q\}}{\text{argmin}}\sum_{q=0}^{M-1}\sum_{l=1}^{S}UB_q^l\\ &s.t.\quad\sum_{q=0}^{M-1}\left\|\mathbf{B}_q\right\|_F^2\leq P_T\\ &\qquad\lambda_1\left(\mathbf{B}_q\mathbf{B}_q^T\right)\leq b_q,\quad 0\leq q\leq M-1,\end{aligned} \tag{31}$$

where the objective function can be written as

$$\begin{aligned}&\sum_{l=1}^{S}UB_q^l=\text{tr}\left(\mathbf{I}_S-\left(\mathbf{E}_{qq,e}^k[0]\mathbf{B}_q\right)^T\right.\\ &\left.\times\left(\mathbf{C}_q+\mathbf{E}_{qq,e}^k[0]\mathbf{B}_q\left(\mathbf{E}_{qq,e}^k[0]\mathbf{B}_q\right)^T\right)^{-1}\mathbf{E}_{qq,e}^k[0]\mathbf{B}_q\right)\\ &=\text{tr}\left(\left(\mathbf{I}_S+\left(\mathbf{E}_{qq,e}^k[0]\mathbf{B}_q\right)^T\mathbf{C}_q^{-1}\mathbf{E}_{qq,e}^k[0]\mathbf{B}_q\right)^{-1}\right).\end{aligned} \tag{32}$$

Although (31) does not match the minimization of the sum MSE, it allows us to benefit from the framework developed in [5]. In this regard, we can state that if the constraints on the dominant eigenvalues are ignored, the solution of (31) has the structure $\mathbf{B}_q=\mathbf{U}_q\Sigma_q$, where $\mathbf{U}_q\in\mathbb{R}^{N_T\times\check{L}_q}$ contains the eigenvectors of $\left(\mathbf{E}_{qq,e}^k[0]\right)^T\mathbf{C}_q^{-1}\mathbf{E}_{qq,e}^k[0]\in\mathbb{R}^{N_T\times N_T}$ that are associated with the $\check{L}_q$ largest eigenvalues. The matrix Σ_q is decomposed as $\Sigma_q=[\mathbf{0}\;\;\mathbf{P}_q]$, where $\mathbf{0}\in\mathbb{R}^{\check{L}_q\times S-\check{L}_q}$ is zero valued and $\mathbf{P}_q=\text{diag}\left\{\sqrt{p_q^{\check{L}_q}},...,\sqrt{p_q^1}\right\}\in\mathbb{R}^{\check{L}_q\times\check{L}_q}$. Whether it is possible or not to spatially multiplex S streams will be given by $\check{L}_q=\min\left(S,\text{rank}\left(\left(\mathbf{E}_{qq,e}^k[0]\right)^T\mathbf{C}_q^{-1}\mathbf{E}_{qq,e}^k[0]\right)\right)$. As a consequence, $\check{L}_q\leq S$. From the precoding structure described above, the constraint on the dominant eigenvalue becomes $\lambda_1\left(\mathbf{B}_q\mathbf{B}_q^T\right)=\max\left\{p_q^1,...,p_q^{\check{L}_q}\right\}\leq b_q$. Then, all

the power coefficients should comply with this inequality $p_q^l \leq b_q$, for $l = 1, ..., \check{L}_q$. Since the additional constraints are linear with the power coefficients, the upper bounds on the dominant eigenvalues do not affect the solvability of the problem (see [5]). Hence, the precoder that solves (31) is given by $\mathbf{B}_q = \mathbf{U}_q \Sigma_q$. As a consequence, the power coefficients are obtained by solving

$$\begin{aligned} &\underset{\{p_q^l\}}{\operatorname{argmin}} \sum_{q=0}^{M-1} \sum_{l=1}^{\check{L}_q} \frac{1}{1+\lambda_q^l p_q^l} \\ &s.t. \quad \sum_{q=0}^{M-1} \sum_{l=1}^{\check{L}_q} p_q^l \leq P_T \\ &\qquad 0 \leq p_q^l \leq b_q, \quad 1 \leq l \leq \check{L}_q, \quad 0 \leq q \leq M-1. \end{aligned} \tag{33}$$

Let λ_q^l be the lth largest eigenvalue of matrix $\left(\mathbf{E}_{qq,e}^k[0]\right)^T \mathbf{C}_q^{-1} \mathbf{E}_{qq,e}^k[0]$. Since the problem (33) is convex, the power coefficients can be formulated as follows:

$$p_q^l = \min\left(\left(\mu^{-1/2}\left(\lambda_q^l\right)^{-1/2} - \left(\lambda_q^l\right)^{-1}\right)^+, b_q\right) \tag{34}$$

where μ is the Lagrange multiplier that guarantees that the total power constraint is active and $(x)^+ = \max(0, x)$. One option to compute (34) is to proceed similarly to the cap-limited water-filling algorithm [28].

In order to find a low-complexity solution we have forced per-stream powers to be lower than $\{b_q\}$, i.e. $p_q^l \leq b_q$. If the coefficients that delimit the allowed values are too high the exact MSE will lie far below with respect to (26). Conversely, if the parameters $\{b_q\}$ take small values, the streams transmitted on the worst subchannels may not receive enough power to overcome the spectral nulls. In this regard, we have empirically observed that when the values of b_q are around $\frac{P_T}{M}$, we achieve a good trade-off. The problem of finding a tight upper bound for $\lambda_1\left(\mathbf{B}_q \mathbf{B}_q^T\right)$ that relies on analytical expressions is not fully explored in this paper and, therefore, it remains open.

B. Refinement of the subband processing

To perform closer to the optimum, we propose to update the receive matrices so that the exact sum MSE is minimized having fixed the transmit processing. In other words, having computed the precoders with (31), the receivers are recalculated to solve (23). Therefore it results in

$$\begin{aligned} \mathbf{A}_{q,e} = \left[\mathbf{a}_{q,e}^1 ... \mathbf{a}_{q,e}^S\right] = (\mathbf{R}_q + \\ \sum_{m=q-1}^{q+1} \sum_{t=-L_a-2}^{L_a+2} \mathbf{E}_{qm,e}^k[t] \mathbf{B}_m \left(\mathbf{E}_{qm,e}^k[t] \mathbf{B}_m\right)^T \Bigg)^{-1} \mathbf{E}_{qq,e}^k[0] \mathbf{B}_q. \end{aligned} \tag{35}$$

Note that matrix inversion is allowed since it is assumed that the noise autocorrelation matrix is full rank. By using this equality $\mathbf{A} = \left(\mathbf{EB}\left(\mathbf{EB}\right)^H + \mathbf{R}\right)^{-1} \mathbf{EB} = \mathbf{R}^{-1}\mathbf{EB}\left(\mathbf{I} + \left(\mathbf{EB}\right)^H \mathbf{R}^{-1}\mathbf{EB}\right)^{-1}$ [5], the MIMO decoding matrix can be expressed as

$$\begin{aligned} \mathbf{A}_{q,e} = \; & \bar{\mathbf{C}}_q^{-1} \mathbf{E}_{qq,e}^k[0] \mathbf{B}_q \\ & \times \left(\mathbf{I}_S + \left(\mathbf{E}_{qq,e}^k[0]\mathbf{B}_q\right)^T \bar{\mathbf{C}}_q^{-1} \mathbf{E}_{qq,e}^k[0]\mathbf{B}_q\right)^{-1} \end{aligned} \tag{36}$$

with

$$\begin{aligned} \bar{\mathbf{C}}_q \; & = \mathbf{R}_q + \sum_{m=q-1}^{q+1} \sum_{t=-L_a-2}^{L_a+2} \mathbf{E}_{qm,e}^k[t] \mathbf{B}_m \\ & \times \left(\mathbf{E}_{qm,e}^k[t]\mathbf{B}_m\right)^T - \mathbf{E}_{qq,e}^k[0]\mathbf{B}_q \left(\mathbf{E}_{qq,e}^k[0]\mathbf{B}_q\right)^T \end{aligned} \tag{37}$$

From here onwards we assume that the equalizers are built as (36) describes if otherwise stated.

C. Widely linear vs. linear processing

In this section we compare a MIMO-FBMC/OQAM system that is based on the proposed WL processing with a MIMO-OFDM system that relies on the linear processing described in [5]. The expressions presented in the following are built on optimistic assumptions for the ease of the tractability when FBMC/OQAM is considered. Thus, the comparison might be unfair. The analysis derived in this section does not allow us to conclude which is the best technique but it allows us to find out in which multi-antenna configurations FBMC/OQAM may remain competitive with OFDM.

In the WL case, the input/output relationship of those symbols transmitted on the qth subband and the time instant of interest will be given by $\mathbf{A}_{q,e}^T \mathbf{E}_{qq,e}^k[0] \mathbf{B}_q$. Unless (30) and (37) coincide, i.e. $\bar{\mathbf{C}}_q = \mathbf{C}_q$, the MIMO channel matrix is not decoupled into independent subchannels. The diagonal structure can be achieved if the additive noise is the dominant source of interference or in the absence of ISI and ICI. Supposing the latter assumption, the noise correlation matrix is formulated as $\bar{\mathbf{C}}_q = \mathbf{C}_q = \mathbf{R}_q = 0.5 N_0 \mathbf{I}_{2N_R}$ (see [12]), provided that we stick to the case that $L_a = 0$ and the noise samples are independent and identically distributed circularly symmetric Gaussian variables, i.e. $w_j[n] \sim \mathcal{CN}(0, N_0)$. In order to make expressions analytically tractable, we consider an interference-free scenario and we focus on the case that the equalizers have no memory, i.e. $L_a = 0$. Then, the signal to interference plus noise ratio (SINR) is given by

$$SINR_q^l = \frac{1}{MSE_q^l} - 1 = \frac{p_q^l \bar{\lambda}_q^l}{0.5 N_0}, \tag{38}$$

where $\bar{\lambda}_q^l$ is the lth largest eigenvalue of matrix $\left(\mathbf{E}_{qq,e}^k[0]\right)^T \mathbf{E}_{qq,e}^k[0]$. We have assumed that $S \leq \operatorname{rank}\left(\left(\mathbf{E}_{qq,e}^k[0]\right)^T \mathbf{E}_{qq,e}^k[0]\right) = \min\left(N_T, 2N_R\right)$. Since (38) corresponds to a fictitious scenario that is interference-free, we can conclude that the exact SINR is upper bounded by (38). Thoroughly examining $\mathbf{E}_{qq,e}^k[0]$ it is possible to approximate its value by $\mathbf{E}_{qq,e}^k[0] \approx \left[\Re\left(\mathbf{H}_q^T\right) \;\; \Im\left(\mathbf{H}_q^T\right)\right]^T = \mathbf{H}_{q,e}$, where $\mathbf{H}_q$ is the frequency response of the MIMO channel matrix evaluated on $\frac{2\pi}{M} q$. To support this statement we first expand this term $g_{qq}^{ij}[0]$, written in (10), as follows:

$$g_{qq}^{ij}[0] = \sum_{t=0}^{L_{ch}-1} h_{ij}[t] \underbrace{\left(\sum_{v=0}^{L-1} p[v]\, p[v+t]\right)}_{r_p[t]} e^{-j\frac{2\pi}{M} qt}. \tag{39}$$

It should be mentioned that $p[v] \neq 0$ for $v = 0, ..., L-1$. The maximum channel excess delay is denoted L_{ch} and

it is assumed equal for all the links. According to [29], the prototype pulse in the discrete-time domain can be obtained by sampling the analog pulse $p(t)$, i.e. $p[v] = p\left((v-0.5(L-1))\,\frac{1}{f_s}\right)$, where f_s is the sampling frequency and the delay $0.5(L-1)$ is chosen to force $p[v]$ to be causal. Then, using the first order Taylor expansion of $p(t)$, we can approximate the samples around the *v*th sampling instant as $p[v+t] \approx p[v] + \frac{t}{f_s} d[v]$, [29]. Writing the derivative of the pulse as $p'(t)$ we define $d[v] = p'\left((v-0.5(L-1))\,\frac{1}{f_s}\right)$. In the FBMC/OQAM context the pulses follow the Nyquist pulse shaping idea, thus they present an even symmetry, which implies that $p[v] = p[L-1-v]$ as it is stated in [10], and consequently $d[v] = -d[L-1-v]$. The discrete-time signal $d[v]$ will present an odd symmetry with respect to the central sample. As a consequence, $r_p[t] \approx \sum_{v=0}^{L-1} |p[v]|^2$. If the prototype pulse is properly scaled to have unit-energy, the value of $g_{qq}^{ij}[0]$ is approximately the element of matrix $\mathbf{H}_q$ located at the *i*th column and *j*th row. This confirms that $\mathbf{E}_{qq,e}^{k}[0] \approx \mathbf{H}_{q,e}$, as long as the number of carriers is sufficiently large (see [29]). From here onwards we assume that $\mathbf{E}_{qq,e}^{k}[0] = \mathbf{H}_{q,e}$ holds true.

At this point, it would be interesting to know how the upper bound in (38) compares with the solution based on the linear processing [5]. To this end, we formulate the SINR in the OFDM case, which is given by

$$SINR_q^l = \frac{2p_q^l \beta_q^l}{N_0}. \tag{40}$$

The variance of the noise is not halved because the technique is designed over the complex field. The factor 2 in the numerator highlights that the real PAM symbols are obtained from in-phase and quadrature components of the QAM symbols, which are transmitted in OFDM systems. The coefficients $\left\{\beta_q^1, ..., \beta_q^S\right\}$ denote the *S* largest non-zero eigenvalues of the matrix $\mathbf{H}_q^H \mathbf{H}_q$, so it becomes clear that the power distribution will be different from that of (38). In OFDM systems the maximum number of streams that can be spatially multiplexed is given by $\text{rank}\left(\mathbf{H}_q^H \mathbf{H}_q\right) = \min(N_T, N_R)$. To carry out a fair comparison with FBMC/OQAM we exclusively consider the schemes where $S \leq \min(N_T, N_R)$. Also notice that $\mathbf{H}_{q,e}^T \mathbf{H}_{q,e} = \Re\left(\mathbf{H}_q^H \mathbf{H}_q\right)$ and $\Im\left(\mathbf{H}_q^H \mathbf{H}_q\right) = \Re\left(\mathbf{H}_q^T\right)\Im\left(\mathbf{H}_q\right) - \Im\left(\mathbf{H}_q^T\right)\Re\left(\mathbf{H}_q\right)$, which highlights that $\sum_{l=1}^{N_T} \beta_q^l = \sum_{l=1}^{N_T} \bar{\lambda}_q^l$. In addition, $\mathbf{c}^T \Im\left(\mathbf{H}_q^H \mathbf{H}_q\right) \mathbf{c} = 0$ for any $\mathbf{c} \in \mathbb{R}^{N_T \times 1}$. In view of the above discussion we can write these inequalities

$$\begin{aligned} \beta_q^1 &= \max_{\|\mathbf{c}\|_2=1} \mathbf{c}^H \mathbf{H}_q^H \mathbf{H}_q \mathbf{c} \geq \left(\mathbf{u}_q^1\right)^H \mathbf{H}_q^H \mathbf{H}_q \mathbf{u}_q^1 = \bar{\lambda}_q^1 \\ \beta_q^{N_T} &= \min_{\|\mathbf{c}\|_2=1} \mathbf{c}^H \mathbf{H}_q^H \mathbf{H}_q \mathbf{c} \leq \left(\mathbf{u}_q^{N_T}\right)^H \mathbf{H}_q^H \mathbf{H}_q \mathbf{u}_q^{N_T} = \bar{\lambda}_q^{N_T}, \end{aligned} \tag{41}$$

when $\mathbf{u}_q^l$ corresponds to the real-valued eigenvector of $\mathbf{H}_{q,e}^T \mathbf{H}_{q,e}$ that is associated to the eigenvalue $\bar{\lambda}_q^l$. With the exception of the two specific cases written in (41), we have not been able to establish any inequality for the rest of eigenvalues. With that, we should set $S = N_T \leq N_R$ to ensure that at least in one spatial subchannel, in particular the *S*th spatial subchannel, the highest gain will take place when the WL filtering is performed, as long as the interference is removed. With an alternative configuration all the spatial subchannels might present the highest gain when OFDM is considered.

IV. Iterative design

The processing developed in Section III gives rise to a suboptimal design. Examining (22) from a different perspective, that is forgetting about the complexity, we can find a local solution that is computed via the alternating optimization method. The idea is to independently optimize receive and transmit matrices in an iterative fashion. The resulting design will be used as a benchmark for the results of Section III. Without making any relaxation the sum MSE is given by

$$\begin{aligned} &MSE\left(\{\mathbf{A}_{q,e}, \mathbf{B}_q\}\right) = \sum_{q=0}^{M-1} \mathbb{E}\left\{\left\|\mathbf{d}_q[k] - \check{\mathbf{d}}_q[k]\right\|_2^2\right\} \\ &= M \times S + \sum_{q=0}^{M-1} \sum_{m=q-1}^{q+1} \sum_{t=-L_a-2}^{L_a+2} \left\|\mathbf{A}_{q,e}^T \mathbf{E}_{qm,e}^k[t] \mathbf{B}_m\right\|_F^2 \\ &+ \sum_{q=0}^{M-1} \text{tr}\left(\mathbf{A}_{q,e}^T \mathbf{R}_q \mathbf{A}_{q,e} - 2\mathbf{A}_{q,e}^T \mathbf{E}_{qq,e}^k[0] \mathbf{B}_q\right). \end{aligned} \tag{42}$$

The cost function in (42) is obtained by resorting to this definition $\mathbf{A}_{q,e} = \left[\mathbf{a}_{q,e}^1 ... \mathbf{a}_{q,e}^S\right] \in \mathbb{R}^{2N_R(1+2L_a) \times S}$ and the precoding matrix written in (17). Hence, precoders are restricted to be real-valued. It can be verified that the (*l*th,*l*th) element of $\mathbb{E}\left\{\left\|\mathbf{d}_q[k] - \check{\mathbf{d}}_q[k]\right\|_2^2\right\}$ coincides with (23).

A. Receiver design

The receiver design hinges on minimizing (42) for fixed MIMO precoding matrices. Then, the optimal equalizers are

$$\begin{aligned} \mathbf{A}_{q,e} \quad &= \left(\mathbf{R}_q + \sum_{m=q-1}^{q+1} \sum_{t=-L_a-2}^{L_a+2} \mathbf{E}_{qm,e}^k[t] \mathbf{B}_m \right. \\ &\left. \times \left(\mathbf{E}_{qm,e}^k[t] \mathbf{B}_m\right)^T\right)^{-1} \mathbf{E}_{qq,e}^k[0] \mathbf{B}_q. \end{aligned} \tag{43}$$

B. Transmitter design

The transmitter design is challenging because of the total power constraint. Given the equalizers, the problem becomes

$$\begin{aligned} &\underset{\{\mathbf{B}_q\}}{\text{argmin}}\, MSE\left(\{\mathbf{A}_{q,e}, \mathbf{B}_q\}\right) \\ &s.t. \quad \sum_{q=0}^{M-1} \|\mathbf{B}_q\|_F^2 \leq P_T. \end{aligned} \tag{44}$$

Notice that (44) is convex and satisfies the Slater's constraint qualification [30], thus we can resort to the dual optimization framework to solve the primal problem. Based on that, we first generate the Lagrangian function as follows:

$$\begin{aligned} L\left(\lambda, \{\mathbf{A}_{q,e}, \mathbf{B}_q\}\right) \quad &= MSE\left(\{\mathbf{A}_{q,e}, \mathbf{B}_q\}\right) \\ &+ \lambda\left(\sum_{q=0}^{M-1} \|\mathbf{B}_q\|_F^2 - P_T\right) \end{aligned} \tag{45}$$

where λ accounts for the Lagrange multiplier. The dual function is obtained by solving

$$g(\lambda) = \min_{\{\mathbf{B}_q\}} L\left(\lambda, \{\mathbf{A}_{q,e}, \mathbf{B}_q\}\right), \tag{46}$$

which allows us to pose the dual problem in this form

$$g(\lambda_{opt}) = \begin{array}{l} \max\limits_{\lambda} g(\lambda) \\ s.t. \quad \lambda \geq 0. \end{array} \tag{47}$$

The MIMO precoding matrix that solves (46) is given by

$$\mathbf{B}_q^*(\lambda) = \left(\sum_{m=q-1}^{q+1} \sum_{t=-L_a-2}^{L_a+2} \left(\mathbf{E}_{mq,e}^k[t]\right)^T \mathbf{A}_{m,e} \times \mathbf{A}_{m,e}^T \mathbf{E}_{mq,e}^k[t] + \lambda \mathbf{I}_{N_T} \right)^{-1} \left(\mathbf{E}_{qq,e}^k[0]\right)^T \mathbf{A}_{q,e}. \tag{48}$$

Plugging λ_{opt} into (48) yields the optimal precoder. In this sense, we propose to compute the optimal Lagrange multiplier by performing a bisection search assuming that $\lambda \in [0 \;\; \lambda_{max}]$. The criterion to bisect the plane is based on evaluating the supragradient of the dual function since it might not be differentiable [31]. The authors in [32] have demonstrated that the dual function can be upper bounded as follows:

$$g(\bar{\lambda}) \leq g(\lambda) + (\bar{\lambda} - \lambda) \left(\sum_{q=0}^{M-1} \left\| \mathbf{B}_q^*(\lambda) \right\|_F^2 - P_T \right). \tag{49}$$

From (49) it is easy to identify the supragradient of the dual function, which is given by $\partial g(\lambda) = \sum_{q=0}^{M-1} \left\| \mathbf{B}_q^*(\lambda) \right\|_F^2 - P_T$. At this point, we should define the initial interval where the Lagrange multiplier lies. Since the strong duality holds, the complementary slackness has to be satisfied [30]. Hence, if $\lambda_{opt} > 0$ the total power constraint is active. By contrast, if the constraint is not satisfied with equality then $\lambda_{opt} = 0$. Bearing the complementary slackness in mind along with the trace inequality $\left(\mathrm{tr}\left(\mathbf{AB}\right) \leq \sum_{i=1}^{N} \lambda_i\left(\mathbf{A}\right) \lambda_i\left(\mathbf{B}\right) \right)$, yields

$$P_T = \sum_{q=0}^{M-1} \left\| \mathbf{B}_q^*(\lambda_{opt}) \right\|_F^2 \leq \sum_{q=0}^{M-1} \sum_{i=1}^{N_T} \frac{\alpha_q^i}{\left(\lambda_{opt} + \gamma_q^{N_T+1-i}\right)^2} \leq \sum_{q=0}^{M-1} \sum_{i=1}^{N_T} \frac{\alpha_q^i}{\lambda_{opt}^2}, \tag{50}$$

for $\lambda_{opt} > 0$. Therefore

$$0 \leq \lambda_{opt} \leq \sqrt{\frac{1}{P_T} \sum_{q=0}^{M-1} \left\| \mathbf{A}_{q,e}^T \mathbf{E}_{qq,e}^k[0] \right\|_F^2} = \lambda_{max}. \tag{51}$$

This result follows from defining the eigenvalues of matrices $\left(\mathbf{E}_{qq,e}^k[0]\right)^T \mathbf{A}_{q,e} \mathbf{A}_{q,e}^T \mathbf{E}_{qq,e}^k[0]$ and

$$\sum_{m=q-1}^{q+1} \sum_{t=-L_a-2}^{L_a+2} \left(\mathbf{E}_{mq,e}^k[t]\right)^T \mathbf{A}_{m,e} \mathbf{A}_{m,e}^T \mathbf{E}_{mq,e}^k[t] \tag{52}$$

as $\left\{\alpha_q^1, ..., \alpha_q^{N_T}\right\}$ and $\left\{\gamma_q^1, ..., \gamma_q^{N_T}\right\}$, respectively. The eigenvalues collected in both sets are arranged in descending order. Setting the upper bound according to (51) certifies that the optimal Lagrange multiplier is confined in the selected interval. The authors have demonstrated in [33] that $\mathbf{B}_q^*(\lambda)$ decreases monotonically with λ. Hence, if $\partial g(0) < 0$, then $\partial g(\lambda) < 0$ for any $\lambda \in [0 \;\; \lambda_{max}]$. Consequently $\lambda_{opt} = 0$ if $\partial g(0) < 0$. Taking this result into account, the Algorithm 1 enables us to perform as close to the optimal value as desired.

Algorithm 1 Precoder design

1: **if** $\partial g(0) < 0$ **then** $\lambda = 0$
2: **else**
3: Set l=0, u=λ_{max}
4: **repeat**
5: $\lambda = 0.5(l + u)$
6: **if** $\partial g(\lambda) < 0$ **then** u = λ **else** l = λ
7: **until** $\sum_{q=0}^{M-1} \left\| \mathbf{B}_q^*(\lambda) \right\|_F^2 \in [\delta P_T \;\; P_T], \quad 0 < \delta < 1$
8: **end if**
9: $\mathbf{B}_q = \mathbf{B}_q^*(\lambda), \quad 0 \leq q \leq M-1$

The algorithm stops when the desired precision is reached. In this paper we fix $\delta = 0.99$. It is important to remark that through a different reasoning we have arrived at the same result as [33]. The overall algorithm operates as the Algorithm 2 describes. At each iteration the sum MSE decreases because the design of precoders and equalizers is governed by the same objective function. Hence, the Algorithm 2 converges to a minimum point since the sum MSE is lower bounded by zero [33]. However, we cannot state that the solution is a global optimum point because (42) is not jointly convex in $\{\mathbf{B}_q\}$ and $\{\mathbf{A}_{q,e}\}$.

Algorithm 2 Alternating optimization method

1: Initialize $\mathbf{A}_{q,e}, \mathbf{B}_q \quad 0 \leq q \leq M-1$
2: **for** i=1,...,N **do**
3: Compute $\mathbf{A}_{q,e}$ using (43)
4: Compute $\mathbf{B}_q$ executing the Algorithm 1
5: **end for**

V. Simulation results

This section evaluates the system performance of the proposed techniques in terms of BER against the average energy symbol to noise ratio, which is defined as $\frac{E_s}{N_0} = \frac{M+CP}{M} \frac{2 \times P_T}{M \times N_0}$. The factor 2 in the numerator accounts for the energy of a complex QAM symbol, since the PAM symbols have unit-energy. It must be mentioned that the FBMC/OQAM modulation does not transmit redundancy, thus $CP = 0$. As for the benchmark, we have simulated the solution that minimizes the sum MSE derived in [5]. The solution can be implemented either in an OFDM or in a FBMC/OQAM architecture, as proposed in [11]. To differentiate each case we use these two acronyms: MSE (OFDM) and MSE (FBMC). Since the non-iterative technique that is described in Section III is based on a real-valued representation of the system model, it is identified in the figures as R-MSE (FBMC). Regarding the system parameters and the propagation conditions, two different scenarios are considered. In scenario 1 the B =10 MHz bandwidth is split into $M = 1024$ carriers and the sampling frequency is set to $f_s = 11.2$ MHz. The propagation conditions obey the ITU Vehicular A channel model. In the scenario 2 the bandwidth and the sampling frequency keep unchanged but the number of carriers is halved, i.e. $M = 512$, and the propagation

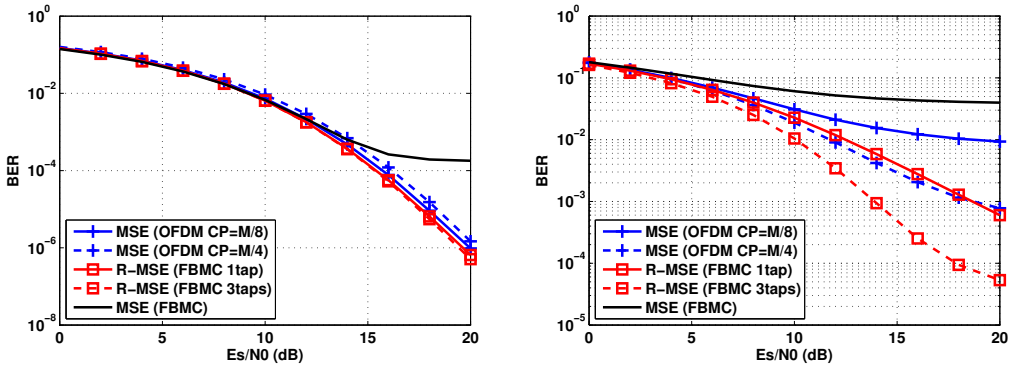

(a) Scenario 1 (b) Scenario 2

Figure 2. BER against $\frac{E_s}{N_0}$ for a 4x2 MIMO communication system. The number of streams transmitted over each subband is $S = 2$. The spectral efficiency values are in bits/s/Hz: (FBMC)=6.615, (OFDM CP=M/8)=5.6 and (OFDM CP=M/4)=5.04.

conditions obey the ITU Vehicular B channel model. Channel models are designed following the guidelines provided in [34].

It is important to remark that only M_a out M subbands are active. In the OFDM case M_a is equal to 720 and 360 in scenario 1 and 2, respectively. By contrast, the reduced out-of-band radiation exhibited by the FBMC/OQAM modulation enables us to reduce the guard bands at the edges of the frequency band. Among the possible prototype pulses that can be used in the FBMC/OQAM modulation, we favour the design based on the frequency sampling approach with an overlapping factor equal to 4, [24]. This translates into the utilization of 756 carriers in the scenario 1 and 378 in the scenario 2, [35]. In all the simulations the symbols are drawn from the 16QAM constellation. This means that the real symbols $\left\{d_q^l[k]\right\}$ are 4PAM. According to the features of the system, the spectral efficiency is $\eta = \frac{S\times M_a\times 2\times f_s}{B\times 0.5\times M} = S3.3075$ bit/s/Hz, when FBMC/OQAM is considered. The term S denotes the number of streams transmitted over each subband. In the OFDM context, the spectral efficiency is $\eta = \frac{S\times M_a\times 4\times f_s}{B\times (M+CP)}$ bit/s/Hz. By setting $CP = \frac{M}{8}$ we obtain $\eta = S2.8$ bit/s/Hz. If the cyclic prefix is extended to $CP = \frac{M}{4}$, the spectral efficiency becomes $\eta = S2.52$ bit/s/Hz. It is worth mentioning that the spectral efficiency expresses the information rate that is transmitted over a given bandwidth.

When the transmission is done over a $N_R \times N_T$ MIMO channel, the receiver and the transmitter have N_R and N_T antennas, respectively. For the simulations, the number of streams and the number of antennas are related as follows: $S = N_T \leq N_R$. The justification is provided in Section III-C. In particular, we focus on the configuration 4x2.

A. BER evaluation under perfect CSI

First we show some results when the CSI is perfectly known. The results depicted in Fig. 2a show that the proposed technique slightly outperforms OFDM. This implies that the R-MSE technique succeeds in removing the interferences as well as the loss in the first subchannel is compensated by the improvement of the second spatial subchannel. The gap between R-MSE and MSE (OFDM) is also due to the energy wastage that implies transmitting the CP. The BER curves of Fig. 2a also highlight that the proposed technique does not benefit from implementing a multi-tap linear equalizer. Therefore, we can state that the channel frequency response is approximately flat at the subcarrier level. As for the MSE (FBMC) technique, it provides satisfactory results at high and moderate noise regime. However, for $\frac{E_s}{N_0} \geq 14$dB the performance starts degrading because the interferences are not removed and as a consequence the BER plot exhibits an error floor when the noise is not the dominant source of interference. The scenario 2 is very challenging because the CP is not long enough to absorb the maximum channel excess delay. As Fig. 2b shows, the larger is the CP, the lower is the BER. The MSE (FBMC) technique does not compare favourably even at high noise regime. Now, the multi-tap linear equalization does push down the BER curves with respect to the single-tap case. The reason lies in the fact that the channel frequency response cannot be modeled flat at the subcarrier level. We have not increased the number of taps beyond 3 because it does not significantly improve the results. The reason is because most of the energy of the interferences comes from the first and second order neighbours. Under the conditions of the scenario 2, the R-MSE technique provides the best results because it is able to cope with the loss of orthogonality.

To evaluate how close the designs addressed in Section III and IV perform, we have tested both schemes in Fig. 3. In particular, we focus on a 4x2 MIMO communication system fixing $\frac{E_s}{N_0}$=20dB. The number of taps of the equalizers is set to 3 and the iterative design is initialized with random matrices. As Fig. 3 shows, the BER achieved by the iterative design decreases as the number of iterations increase. It only outperforms the one-shot design after performing 100 iterations. Beyond that point the improvement is marginal, thus we can conclude that the non-iterative design almost gives the same BER when compared to the value at which the alternating optimization method converges.

B. BER evaluation under imperfect CSI

In real systems the knowledge of the channel is only available through an estimation, which is not perfectly matched to

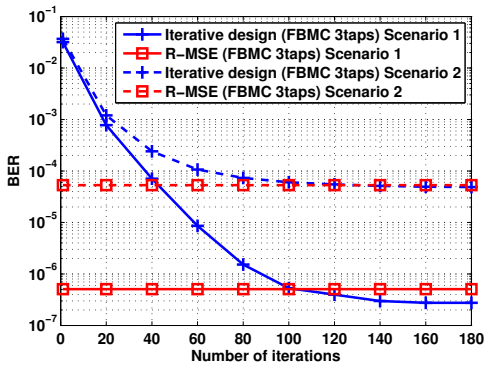

Figure 3. BER for a 4x2 MIMO communication system having fixed $\frac{E_s}{N_0}$=20dB. The number of streams transmitted over each subband is $S = 2$.

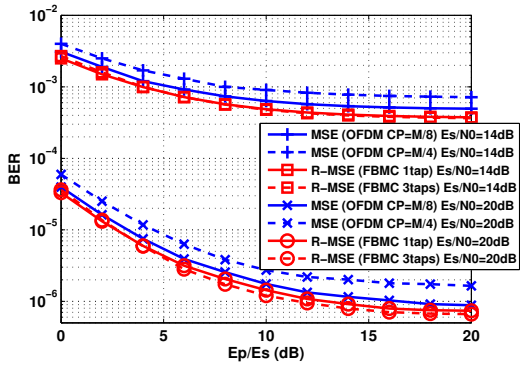

Figure 4. BER against $\frac{E_p}{E_s}$ for a 4x2 MIMO communication system under the propagation conditions of the scenario 1.

the real CSI. To determine the sensitivity to the channel uncertainty we simulate the BER achieved by the MSE (OFDM) and the R-MSE techniques when the channel impulse response is estimated. While the FBMC/OQAM modulation scheme uses the estimator described in [12], the OFDM technique implements the method addressed in [36]. In both cases the training data consists of $\frac{M}{8}$ pilot symbols, which are arranged in a sparse preamble. In Fig. 4 the BER is computed against the energy pilot to the average energy symbol ratio, which is defined as $\frac{E_p}{E_s} = \frac{E_p M}{2P_T}$ where E_p is the energy pilot. Note that $\frac{E_s}{N_0}$ is fixed to 14 dB and 20 dB. The system parameters and the propagation conditions have been chosen according to the scenario 1. The plots depicted in Fig. 4 indicate that the energy pilot has to be boosted with respect to the average energy symbol if we want to perform close to the ideal case, both in the FBMC/OQAM and the OFDM case. However, the most interesting conclusion is that the proposed technique is not more sensitive to the channel uncertainty than the benchmark. As a result, the gap between FBMC/OQAM and OFDM observed in Fig. 2a is maintained. These results provide evidence that MIMO-FBMC/OQAM is as much robust as MIMO-OFDM to the noisy channel estimation.

VI. Conclusions

In this paper we have tackled the joint design of MIMO precoding and decoding matrices for FBMC/OQAM systems under highly frequency selective channels. It is worth mentioning that the non-circular nature exhibited by the OQAM symbols has not been ignored. This has revealed the convenience of performing a WL filtering. Regarding the objective function, we have opted for the minimization of the sum MSE for a given global power budget. Due to the difficulty of solving the original problem, we have replaced the objective function by an upper bound, which poses a problem easier to solve. Simulation-based results show that the proposed solution clearly outperforms existing MIMO-FBMC/OQAM schemes in terms of BER. This work also demonstrates that FBMC/OQAM compares favourably to OFDM as long as the number of streams transmitted over each subband and the number of antennas deployed at each side satisfy this relation: $S = N_T \leq N_R$, which has been theoretically justified. Although the comparison in terms of BER is interesting, the decision that tips the balance towards OFDM or FBMC/OQAM may be determined by other aspects such as the synchronization requirements. Having said that, it must be mentioned that the numerical results highlight that FBMC/OQAM can compete with OFDM even in presence of imperfect CSI. By contrast, in those scenarios where the CP is not long enough to avoid IBI, the FBMC/OQAM modulation scheme shows superior performance than OFDM since the devised subband processing can cope with the loss of orthogonality. Finally, we have demonstrated via simulations that the proposed joint transmit and receive design, which is suboptimal, performs close to a local optimal point that can be reached by means of an alternating optimization method.

Acknowledgment

This work has received funding from the Spanish Ministry of Economy and Competitiveness (Ministerio de Economía y Competitividad) under project TEC2011-29006-C03-02 (GRE3N-LINK-MAC) and from the Catalan Government (2009SGR0891). This work was partially supported by the European Commission through the Emphatic project (ICT-318362).

References

[1] J. Yang and S. Roy, "On joint transmitter and receiver optimization for multiple-input-multiple-output (MIMO) transmission systems," *Communications, IEEE Transactions on*, vol. 42, no. 12, pp. 3221 –3231, dec 1994.

[2] H. Sampath and A. Paulraj, "Joint transmit and receive optimization for high data rate wireless communication using multiple antennas," in *Signals, Systems, and Computers, 1999. Conference Record of the Thirty-Third Asilomar Conference on*, vol. 1, oct. 1999, pp. 215 –219.

[3] H. Sampath, P. Stoica, and A. Paulraj, "Generalized linear precoder and decoder design for MIMO channels using the weighted MMSE criterion," *Communications, IEEE Transactions on*, vol. 49, no. 12, pp. 2198 –2206, dec 2001.

[4] C. H. Ta and S. Weiss, "A Design of Precoding and Equalisation for Broadband MIMO Systems," in *Digital Signal Processing, 2007 15th International Conference on*, july 2007, pp. 571 –574.

[5] D. Palomar, J. Cioffi, and M. Lagunas, "Joint Tx-Rx beamforming design for multicarrier MIMO channels: a unified framework for convex optimization," *Signal Processing, IEEE Transactions on*, vol. 51, no. 9, pp. 2381 – 2401, sept. 2003.

[6] N. Moret, A. Tonello, and S. Weiss, "MIMO Precoding for Filter Bank Modulation Systems Based on PSVD," in *Vehicular Technology Conference (VTC Spring), 2011 IEEE 73rd*, may 2011, pp. 1 –5.

[7] G. Cherubini, E. Eleftheriou, and S. Olcer, "Filtered multitone modulation for very high-speed digital subscriber lines," *Selected Areas in Communications, IEEE Journal on*, vol. 20, no. 5, pp. 1016 –1028, jun 2002.

[8] B. Farhang-Boroujeny, "OFDM Versus Filter Bank Multicarrier," *Signal Processing Magazine, IEEE*, vol. 28, no. 3, pp. 92 –112, may 2011.

[9] B. Saltzberg, "Performance of an efficient parallel data transmission system," *Communication Technology, IEEE Transactions on*, vol. 15, no. 6, pp. 805 –811, december 1967.

[10] P. Siohan, C. Siclet, and N. Lacaille, "Analysis and design of OFDM/OQAM systems based on filterbank theory," *Signal Processing, IEEE Transactions on*, vol. 50, no. 5, pp. 1170 –1183, may 2002.

[11] I. Estella, A. Pascual-Iserte, and M. Payaro and, "OFDM and FBMC performance comparison for multistream MIMO systems," in *Future Network and Mobile Summit, 2010*, june 2010, pp. 1 –8.

[12] M. Caus and A. I. Perez-Neira, "Transmitter-Receiver Designs for Highly Frequency Selective Channels in MIMO FBMC Systems," *Signal Processing, IEEE Transactions on*, vol. 60, no. 12, pp. 6519 –6532, dec. 2012.

[13] M. El Tabach, J.-P. Javaudin, and M. Helard, "Spatial Data Multiplexing Over OFDM/OQAM Modulations," in *Communications, 2007. ICC '07. IEEE International Conference on*, june 2007, pp. 4201 –4206.

[14] A. Ikhlef and J. Louveaux, "Per subchannel equalization for MIMO FBMC/OQAM systems," in *Communications, Computers and Signal Processing, 2009. PacRim 2009. IEEE Pacific Rim Conference on*, aug. 2009, pp. 559 –564.

[15] R. Zakaria, D. Le Ruyet, and M. Bellanger, "Maximum likelihood detection in spatial multiplexing with FBMC," in *Wireless Conference (EW), 2010 European*, april 2010, pp. 1038 –1041.

[16] R. Zakaria and D. Le Ruyet, "A novel FBMC scheme for Spatial Multiplexing with Maximum Likelihood detection," in *Wireless Communication Systems (ISWCS), 2010 7th International Symposium on*, sept. 2010, pp. 461 –465.

[17] ——, "On Maximum Likelihood MIMO detection in QAM-FBMC systems," in *Personal Indoor and Mobile Radio Communications (PIMRC), 2010 IEEE 21st International Symposium on*, sept. 2010, pp. 183 –187.

[18] E. Kofidis and A. Rontogiannis, "Adaptive BLAST decision-feedback equalizer for MIMO-FBMC/OQAM systems," in *Personal Indoor and Mobile Radio Communications (PIMRC), 2010 IEEE 21st International Symposium on*, sept. 2010, pp. 841 –846.

[19] R. Zakaria and D. Le Ruyet, "On spatial data multiplexing over coded filter-bank multicarrier with ML detection," in *Personal Indoor and Mobile Radio Communications (PIMRC), 2011 IEEE 22nd International Symposium on*, sept. 2011, pp. 1391 –1395.

[20] ——, "Partial ISI cancellation with viterbi detection in MIMO filter-bank multicarrier modulation," in *Wireless Communication Systems (ISWCS), 2011 8th International Symposium on*, nov. 2011, pp. 322 –326.

[21] T. Ihalainen, A. Ikhlef, J. Louveaux, and M. Renfors, "Channel Equalization for Multi-Antenna FBMC/OQAM Receivers," *Vehicular Technology, IEEE Transactions on*, vol. 60, no. 5, pp. 2070 –2085, jun 2011.

[22] R. Zakaria and D. Le Ruyet, "A Novel Filter-Bank Multicarrier Scheme to Mitigate the Intrinsic Interference: Application to MIMO Systems," *Wireless Communications, IEEE Transactions on*, vol. 11, no. 3, pp. 1112 –1123, march 2012.

[23] R. Zakaria, D. L. Ruyet, and Y. Medjahdi, "On ISI cancellation in MIMO-ML detection using FBMC/QAM modulation," in *ISWCS*, 2012, pp. 949–953.

[24] M. Bellanger, "Specification and design of a prototype filter for filter bank based multicarrier transmission." ICASSP, 2001, pp. 2417–2420.

[25] A. Viholainen, T. Ihalainen, T. H. Stitz, M. Renfors, and M. Bellanger, "Prototype filter design for filter bank multicarrier transmission," in *in Proceedings of the European Signal Processing Conference (EUSIPCO 2009)*, august 2009.

[26] B. Picinbono and P. Chevalier, "Widely linear estimation with complex data," *Signal Processing, IEEE Transactions on*, vol. 43, no. 8, pp. 2030 –2033, aug 1995.

[27] C. R. Horn, R. A.; Johnson, *Matrix Analysis*. Cambridge University Press, 1985.

[28] N. Papandreou and T. Antonakopoulos, "Bit and power allocation in constrained multicarrier systems: the single-user case," *EURASIP J. Adv. Signal Process*, vol. 2008, Jan. 2008.

[29] X. Mestre, M. Sanchez-Fernandez, and A. Pascual-Iserte, "Characterization of the distortion of OFDM/OQAM modulations under frequency selective channels," in *Signal Processing Conference (EUSIPCO), 2012 Proceedings of the 20th European*, aug. 2012, pp. 1598 –1602.

[30] S. Boyd and L. Vandenberghe, "Convex optimization. 2004," 2004.

[31] S. Boyd, "Ee364b: Lecture slides and notes." [Online]. Available: http://www.stanford.edu/class/ee364b/.

[32] W. Yu and R. Lui, "Dual methods for nonconvex spectrum optimization of multicarrier systems," *Communications, IEEE Transactions on*, vol. 54, no. 7, pp. 1310 –1322, july 2006.

[33] H. Park, S.-H. Park, H.-B. Kong, and I. Lee, "Weighted Sum MSE Minimization under Per-BS Power Constraint for Network MIMO Systems," *Communications Letters, IEEE*, vol. 16, no. 3, pp. 360 –363, march 2012.

[34] "Guidelines for the evaluation of radio transmission technologies for IMT-2000." Recommendation ITU-R M.1225, 1997.

[35] Q. Bai, N. Passas, and J. Nossek, "Scheduling and resource allocation in ofdm and fbmc systems: An interactive approach and performance comparison," in *Wireless Conference (EW), 2010 European*, april 2010, pp. 1042 –1050.

[36] Z. Wu, J. He, and G. Gu, "Design of optimal pilot-tones for channel estimation in MIMO-OFDM systems," in *Wireless Communications and Networking Conference, 2005 IEEE*, vol. 1, march 2005, pp. 12 – 17 Vol. 1.

Màrius Caus (IEEE S'11) received his M.Sc. Telecommunications engineering degree from the Universitat Politècnica de Catalunya (UPC), Barcelona, Spain, in 2008. From February 2009 to June 2009 he worked as a research assistant at Centre Tecnològic de Telecomunicacions de Catalunya (CTTC), Castelldefels, Spain. In September 2009 he was granted by the Spanish Government to carry out his PhD studies in the Signal Theory and Communications Department, UPC. His main research interests include filter bank multicarrier systems, array signal processing and satellite communications.

Ana I. Pérez-Neira (IEEE S'92, M'95, SM'02) is full professor at UPC (Technical University of Catalonia) in the Signal Theory and Communication department. Her research field is signal processing applied to wireless communications (both mobile and satellite). She has been the leader of 20 projects (9 international and 11 national). She is author of more than 40 journal papers (SCI indexed) and more than 150 conference papers (20 invited). She is co-author of 4 books and 5 patents. She has been in the board of directors of ETSETB (Telecom Barcelona) from 2000–03 and currently she is in the board of directors of CTTC (Centre Tecnològic de Telecomunicacions de Catalonia). She is member of Eurasip BoD (European Signal Processing Association) and of IEEE SPTM (Signal Processing Theory and Methods). She has been the visiting professor at KTH (Royal Institute Stockholm) for 6 months and at Shandong University (China) for 1 month. She is the editor of JASP (Journal of Advances in Signal Processing of Hindawi) and reviewer of various journals and organizations. She has chaired 2 international conferences, IWCLD09 and EUSIPCO 2011, and participated in the organization of other 2 (ESA conference'96, SAM'04). Currently, she is Vice Chancellor at UPC.